

COMMUNICATION



Cite this: *Chem. Commun.*, 2019, 55, 8329

Received 23rd April 2019,
Accepted 20th June 2019

DOI: 10.1039/c9cc03139a

rsc.li/chemcomm

Spectral counterstaining in luminescence-enhanced biological Raman microscopy†

Radek Pelc, ^a Vlastimil Mašek, ^b Vicent Llopis-Torregrosa, ^a Petr Bouř ^a
and Tao Wu ^{*a}

Cell imaging heavily depends on fluorescent labels typically incompatible with Raman microscopy. The europium(III) complex based on dipicolinic acid (DPA) presented here is an exception from this rule. Although its luminescence bands are very narrow, their intensity is comparable to the background Raman bands. This makes it complementary to less luminous compounds referred to as Raman tags. Through several examples we show that the complex provides a morphological context in otherwise unstained cells, thus acting as a spectral-counterstaining agent.

In a typical cell-imaging scenario, a particular organic dye specifically accumulates in the structures of interest, such as cell nuclei. Sometimes, so-called counter-staining with another agent is additionally applied. The aim is either to make the already stained structures, for example, chromosomes, better visible,¹ or to stain some of the other structures such as cell or tissue borders.² The latter option provides a morphological context, facilitates navigation in the specimen, and helps to interpret the images.

Because the cell-imaging techniques are dominated by fluorescence microscopy, lanthanide(III) probes have generated considerable interest owing to their unique electronic structure and sensitivity.^{3–7} Their luminescence technically belongs to a gray zone between fluorescence and phosphorescence. It can be greatly enhanced by surrounding the lanthanide core by suitable ligands, generating a so-called antenna effect.³

Label-free imaging requires no staining and thus represents a convenient alternative. Apart from phase-contrast microscopy⁸ and other optical-contrasting modalities, it includes Raman microscopy (“chemical imaging”) capable of identifying certain chemical species in living cells based on their specific spectral bands.⁹ However, as all molecules exhibit Raman scattering to

some extent, many bands overlap, and useful signals can be hidden in an unspecific background. This often makes navigation in Raman images so difficult that they cannot compete with those generated by using either labelled antibodies in immunocytochemical analyses, or recombinant fluorescent proteins such as green, yellow or red fluorescent protein (GFP, YFP or RFP) tagged to (co-expressed with) specific proteins in living cells.¹⁰

It may thus be convenient to combine detailed chemical imaging with staining. However, organic fluorescent dyes typically cannot be used to (counter)stain the specimen because their emission bands are much broader and stronger than the Raman ones. As a result, the Raman image is usually masked by them, and only autofluorescence (typically weak and not very specific) can be employed.¹¹ Haematoxylin-eosin may also be used but only without resins (mounting media).¹²

Compared to fluorescent probes, phosphorescent ones may be more compatible with Raman microscopy. Indeed, a ruthenium-based phosphorescent probe of this kind has been reported.¹³ However, the spectral separation between the Raman and phosphorescence signals is too big to make the probe practically usable, as they can hardly be detected simultaneously in commonly used spectrometers.

A very efficient way to circumvent the band-overlap problem in Raman imaging is based on chemical species or groups referred to as Raman tags. These are designed to generate strong spectral lines in the ‘silent’ range (*ca.* 1800–2800 cm⁻¹) where biomolecules typically do not generate a measurable signal.^{14–18} The tags thus make it possible to follow the metabolism of drugs, proteins, lipids, DNA or glucose in living cells.¹⁴ For example, alkyne-tagged deoxyuridine (an analogue of thymidine) is incorporated into DNA only during its synthesis, and cell proliferation can be monitored by Raman microscopy. Without it, the attachment of the tag is only possible after fixing the cells, *i.e.*, live-cell imaging is ruled out.¹⁵

The Raman tags may be viewed as a spectroscopic alternative to their better known biological counterparts, the above-mentioned recombinant fluorescent proteins.¹⁰ So far, only non-luminescent Raman tags have been reported.^{14–18} Their vibrational Raman

^a *Institute of Organic Chemistry and Biochemistry, Czech Academy of Sciences, Flemingovo náměstí 2, 16610 Prague 6, Czech Republic. E-mail: wu@uochb.cas.cz*

^b *Institute of Molecular and Translational Medicine, Faculty of Medicine and Dentistry, Palacký University, Hněvotínská 5, 77900 Olomouc, Czech Republic*

† Electronic supplementary information (ESI) available: Experimental details including cells, labelling by Eu-DPA complex, and microscopy. See DOI: 10.1039/c9cc03139a

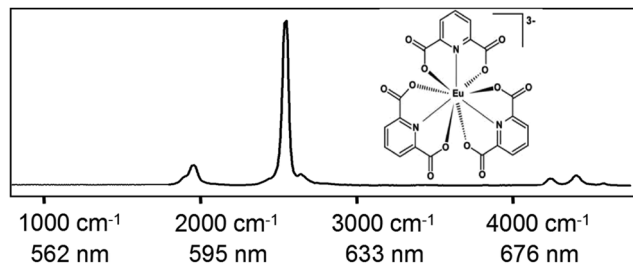


Fig. 1 The dipicolinic acid based europium(III) complex (Eu-DPA) and its luminescence bands in the Raman spectrum obtained at 532 nm excitation.

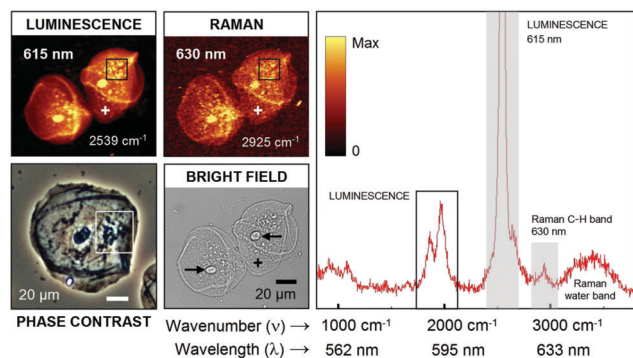


Fig. 2 Freshly isolated human buccal epithelial cells. The Eu-DPA complex mainly labels the nuclei (arrows). A typical luminescence/Raman spectrum shown on the right was obtained at the spot marked "+". The boxed objects are probably bacteria. Objectives, $\times 10/0.25$ (phase contrast) and $\times 50/0.80$ (all other images).

scattering is usually very weak compared to luminescence, implying limited sensitivity in detecting intracellular structures or chemical species.

Lanthanide probes have also been used to label living cells^{3,4,19,20} but to the best of the authors' knowledge, none of them has been demonstrated yet as suitable for Raman microscopy. A frequently encountered problem is their instability in the aqueous environment.

The aim of the present study is to explore the possibility of combining luminescence and Raman microscopy, with the aid of a water-soluble, dipicolinic acid-based europium(III) complex further referred to as "Eu-DPA". As analysed elsewhere, Eu-DPA luminescence bands observed in the Raman spectrum are intense, narrow, and often outside the region typical for the vibrational transitions (Fig. 1).^{21,22}

As shown in Fig. 2 and 3, in buccal epithelial and HeLa cells, the Eu-DPA complex accumulated mostly in nuclei and nucleoli, respectively, as verified by phase-contrast images. Slightly defocused, contrast-optimized bright-field images could also be used in Fig. 3.

This preference for the nuclei seems to be one of the characteristics of the Eu^{III} complexes. They internalize in nucleoli,¹⁹ as do phosphorescent heavy-metal (non-lanthanide)²³ and fluorescent ruthenium complexes.²⁴ Our results demonstrate that some structures outside the nuclei are also labelled by Eu-DPA, even though much less prominently.

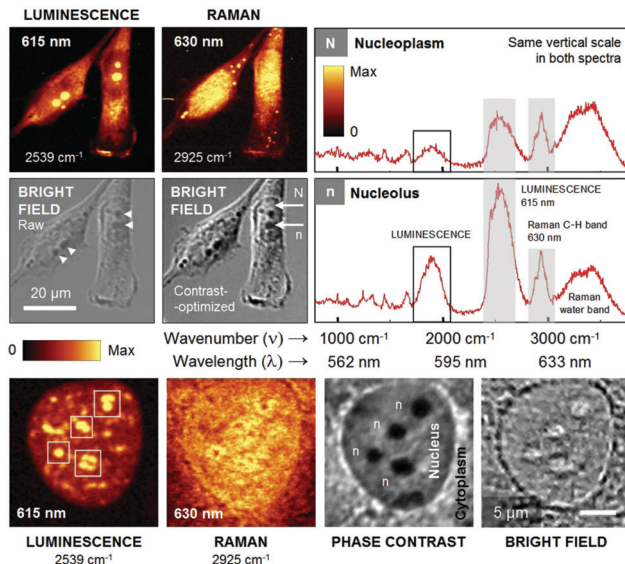


Fig. 3 Live-stained HeLa cells (post-fixed). At the top, luminescence/Raman and bright-field images are shown, with spectra (to scale) recorded from the nucleoplasm (N) and nucleolus (n). The nucleoli are marked by arrowheads in the bright field images. At the bottom, the nucleus of another cell is displayed in detail. Objectives, $\times 50/0.80$ (top panel), $\times 60/1.0$ W (bottom panel except phase contrast) and $\times 40/0.75$ (phase contrast).

The affinity of the complex to nuclei and nucleoli will be the subject of future research (including the use of highly specific nucleolar dyes¹⁹) as it may be medically relevant. For example, in human buccal epithelial cells, an increased number of micronuclei and adherent bacteria correlates with a higher incidence of cancer.²⁵ In such tiny structures, a strong luminescence signal would be instrumental even if partly masking smaller Raman peaks, as in Fig. 2. As only certain structures inside the nucleoli of HeLa cells seem to be labelled by Eu-DPA (*cf.* Fig. 3) the complex may be labelling only a certain subset of chemical species present in this organelle, possibly a major nucleolar protein fibrillarin.²⁶ Nucleolar compartmentalization has important implications for regulation of RNA synthesis (transcription).²⁷

The intine of a pollen grain of juniper consists of two cells, bigger vegetative and smaller generative. Judging by cell shape and size, the complex probably stained the generative cell (Fig. 4) while the Raman signal of the C-H stretching band highlighted the vegetative cell, *i.e.*, the luminescence and Raman signals are complementary. In this particular case, they are also comparable in magnitude; the luminescence line (615 nm) is as strong as the main Raman (C-H stretching) band (630 nm). The Eu-DPA concentration was 1.6 mM, which well documents the convenience of the current protocol. For example, the Raman band of a conventional alkyne deoxyuridine Raman tag is about two orders of magnitude weaker.¹⁸

In yeast, very little of the Eu-DPA complex was found inside the cells themselves, and it was mostly highlighting the cell wall and presumably also the periplasmic space (Fig. 5). This may be attributed to preferential binding of the Eu-DPA complex to the polysaccharide-rich cell-wall components or its inability to cross the plasmalemma into the cytosol. At the very least, the

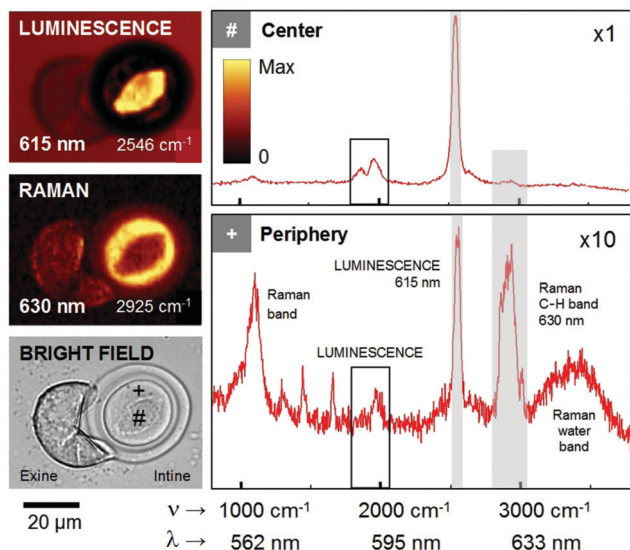


Fig. 4 Hydrated pollen grains of juniper (*Juniperus chinensis*). The central part strongly labelled by the Eu-DPA complex probably colocalizes with a generative cell. Note complementary rendering by the closely separated luminescence (615 nm) and Raman (630 nm) signals. The Raman band at 564 nm ($\sim 1100\text{ cm}^{-1}$) may be assigned to polysaccharides present in high amounts in pollen grains as storage substances. Objective, $\times 50/0.80$.

complex makes it easier to visualize the cell wall in the same cell studied by Raman microscopy. This would be advantageous especially if the cell wall itself is the object of investigation.²⁸ Cell wall thickness is an important parameter reflecting metabolic conditions and possibly affecting drug uptake. It depends on composition of the extracellular medium. In our case, the cell wall is not discernible at all in a Raman image generated from the main C–H stretching band at 630 nm (Fig. 5). Bright-field images are of limited use here because the contrast in them strongly varies with position of the focal plane. Likewise, phase-contrast images suffer from so-called ‘halo’/shade-off artifacts⁸ preventing the correct visualization of structures close to the cell border, unless inspecting very thin cells (Fig. 2), or *e.g.* pseudopodia or lamellipodia.

A detailed assignment and discrimination of the luminescence and Raman bands can be found, for example in our previous study devoted to a water-insoluble europium(III) complex.²⁹ We also showed that identification of transitions in other luminescent lanthanide compounds can be greatly enhanced by magnetic circularly polarized luminescence experiments.²¹ This was demonstrated for many $\text{Na}_3[\text{Ln}(\text{DPA})_3]$ complexes; Ln = Ce, Pr, Nd, Sm, Eu, Tb, Dy, Ho, and Er.

The Eu-DPA complex itself was proposed to indicate the structure of amino acids, oligopeptides and proteins. For this purpose, the circularly polarized luminescence (CPL) component of the spectra detected by means of Raman optical activity (ROA) spectroscopy proved extremely useful.^{22,30} For example, under 532 nm excitation, characteristic luminescence bands of Eu(III) around 1900 cm^{-1} ($^5\text{D}_0 \rightarrow ^7\text{F}_1$) and 2500 cm^{-1} ($^5\text{D}_0 \rightarrow ^7\text{F}_2$)³⁰ were proposed as marker bands to detect small molecules, as they do not overlap with the vibrational Raman signal of most organic components. Similar compounds have been

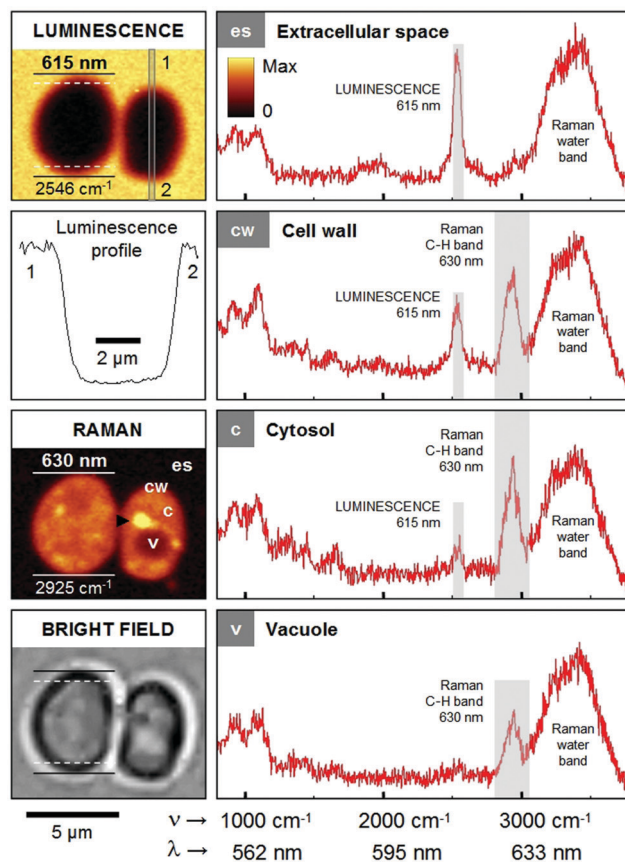


Fig. 5 Yeast cells (*Candida albicans*). As the Eu-DPA complex does not readily enter the cytosol its luminescence mostly highlights the cell wall marked by horizontal lines. A luminescence profile across one of the cells is shown. The bright spot (▶) in the Raman image is a lipid droplet (spectrum not shown). Spectra are to scale. Objective, $\times 60/1.0\text{ W}$.

used to identify saccharides.^{31,32} These studies convincingly showed that the complex specifically interacts with individual biomolecular species. In the future, specific binding, spectroscopic and toxicity properties of the lanthanide complexes will be explored in living cells.

The data obtained with the Eu-DPA complex indicate that simultaneous detection of luminescence and Raman signal opens new possibilities in cell imaging. An important advantage of using the europium(III) complex in Raman microscopy lies in the inherently much stronger luminescence signal, compared to that of vibrational Raman tags. For the samples investigated in the present study, the water-soluble complex provided a much needed morphological context in otherwise unstained cells examined by Raman microscopy, and may be viewed as a spectral-counterstaining substance. A weak point may be that labelling by the complex is less specific, which can be rectified in the future by designing suitable ligands targeted to specific sites in living cells.

TW wishes to express his gratitude to the Embassy of the Czech Republic in Beijing. The authors are grateful to Dr Karel Koberna (IMTM Olomouc) for helping to identify nucleoli and to Dr Olga Heidingsfeld (University of Pardubice) for comments on yeasts. The present study was supported by the Czech Science

Foundation (19-05974Y and 18-05770S) and the Ministry of Education (CZ.02.1.01/0.0/0.0/16_019/0000729, LM2015062, LO1302, LTC17012 and CZ.02.1.01/0.0/0.0/16_019/0000868).

Conflicts of interest

There are no conflicts to declare.

Notes and references

- 1 D. Schwezer, *Hum. Genet.*, 1981, **57**, 1–14.
- 2 C. Kizil, A. Iltzsche, A. K. Thomas, P. Bhattarai, Y. Zhang and M. Brand, *PLoS One*, 2015, **10**, e0124073.
- 3 J. C. G. Bünzli, *J. Lumin.*, 2016, **170**, 866–878.
- 4 E. Mathieu, A. Sipos, E. Demeyere, D. Phipps, D. Sakaveli and K. E. Borbas, *Chem. Commun.*, 2018, **54**, 10021–10035.
- 5 A. J. Amoroso and S. J. A. Pope, *Chem. Soc. Rev.*, 2015, **44**, 4723–4742.
- 6 M. C. Heffern, L. M. Matosziuk and T. J. Meade, *Chem. Rev.*, 2014, **114**, 4496–4539.
- 7 A. T. Frawley, H. V. Linford, M. Starck, R. Pal and D. Parker, *Chem. Sci.*, 2018, **9**, 1042–1049.
- 8 F. Zernike, *Science*, 1955, **121**, 345–349.
- 9 B. Kann, H. L. Offerhaus, M. Windbergs and C. Otto, *Adv. Drug Delivery Rev.*, 2015, **89**, 71–90.
- 10 J. W. Lichtman, J. Livet and J. R. Sanes, *Nat. Rev. Neurosci.*, 2008, **9**, 417–422.
- 11 K. Kong, C. J. Rowlands, S. Varma, W. Perkins, I. H. Leach, A. A. Koloydenko, H. C. Williams and I. Notingher, *Proc. Natl. Acad. Sci. U. S. A.*, 2013, **110**, 15189–15194.
- 12 L. Andronie, V. Mireşan, A. Coroian, I. Pop, C. Răducu, A. Rotaru, D. Cocan, S. C. Pânzaru, I. Domşa and C. O. Coroian, *ProEnviron-ment*, 2015, **8**, 590–600.
- 13 L. Cosgrave, M. Devocelle, R. J. Forster and T. E. Keyes, *Chem. Commun.*, 2010, **46**, 103–105.
- 14 Z. Zhao, Y. Shen, F. Hu and W. Min, *Analyst*, 2017, **142**, 4018–4029.
- 15 A. F. Palonpon, M. Sodeoka and K. Fujita, *Curr. Opin. Chem. Biol.*, 2013, **17**, 708–715.
- 16 J. Ando, M. Asanuma, K. Dodo, H. Yamakoshi, S. Kawata, K. Fujita and M. Sodeoka, *J. Am. Chem. Soc.*, 2016, **138**, 13901–13910.
- 17 H. Yamakoshi, K. Dodo, A. Palonpon, J. Ando, K. Fujita, S. Kawata and M. Sodeoka, *J. Am. Chem. Soc.*, 2012, **134**, 20681–20689.
- 18 H. Yamakoshi, K. Dodo, M. Okada, J. Ando, A. Palonpon, K. Fujita, S. Kawata and M. Sodeoka, *J. Am. Chem. Soc.*, 2011, **133**, 6102–6105.
- 19 E. J. New, D. Parker, D. G. Smith and J. W. Walton, *Curr. Opin. Chem. Biol.*, 2010, **14**, 238–246.
- 20 M. Sy, A. Nonat, N. Hildebrandt and L. J. Charbonnière, *Chem. Commun.*, 2016, **52**, 5080–5095.
- 21 T. Wu, J. Kapitán, V. Andrushchenko and P. Bouř, *Anal. Chem.*, 2017, **89**, 5043–5049.
- 22 E. Brichtová, J. Hudecová, N. Vršková, J. Šebestík, P. Bouř and T. Wu, *Chem. – Eur. J.*, 2018, **24**, 8664–8669.
- 23 Q. Zhao, C. Huang and F. Li, *Chem. Soc. Rev.*, 2011, **40**, 2508–2524.
- 24 N. A. O'Connor, N. Stevens, D. Samaroo, M. R. Solomon, A. A. Marti, J. Dyer, H. Vishwasrao, D. L. Akins, E. R. Kandel and N. J. Turro, *Chem. Commun.*, 2009, 2640–2642.
- 25 N. K. Proia, G. M. Paszkiewicz, M. A. Sullivan Nasca, G. E. Franke and J. L. Pauly, *Cancer Epidemiol., Biomarkers Prev.*, 2006, **15**, 1061–1077.
- 26 M. A. Amin, S. Matsunaga, N. Ma, H. Takata, M. Yokoyama, S. Uchiyama and K. Fukui, *Biochem. Biophys. Res. Commun.*, 2007, **360**, 320–326.
- 27 S. Yildirim, E. Castano, M. Sobol, V. V. Philimonenko, R. Dzijak, T. Venit and P. Hozák, *J. Cell Sci.*, 2013, **126**, 2730–2739.
- 28 H. Noothalapati, T. Sasaki, T. Kaino, M. Kawamukai, M. Ando, H.-O. Hamaguchi and T. Yamamoto, *Sci. Rep.*, 2016, **6**, 27789.
- 29 T. Wu, J. Kapitán, V. Mašek and P. Bouř, *Angew. Chem., Int. Ed.*, 2015, **54**, 14933–14936.
- 30 T. Wu, J. Kessler and P. Bouř, *Phys. Chem. Chem. Phys.*, 2016, **18**, 23803–23811.
- 31 T. Wu, J. Průša, J. Kessler, M. Dračinský, J. Valenta and P. Bouř, *Anal. Chem.*, 2016, **88**, 8878–8885.
- 32 T. Wu, J. Kessler, J. Kaminský and P. Bouř, *Chem. – Asian J.*, 2018, **13**, 3865–3870.